

Towards Bearings Prognostics Based on Oil Debris

Orel Portal¹, Eyal Madar², Renata Klein³, Jacob Bortman⁴, Jeremy Nickell⁵ and Mathew Kirsch⁶

^{1,2,4} PHM Laboratory, Department of Mechanical Engineering, Ben-Gurion University of the Negev, P.O.B 653, Beer-Sheva 8410501, Israel

orelpor@post.bgu.ac.il

eyalma@post.bgu.ac.il

jacbort@post.bgu.ac.il

³R.K. Diagnostics, P.O.B 101, Gilon, D.N. Misgav 20103, Israel

Renata.klein@rkdiagnostics.co.il

^{5,6}Aerospace Systems Directorate, Air Force Research Laboratory, Wright-Patterson Air Force Base, OH 45433, USA

jeremy.nickell@us.af.mil

mathew.kirsch@us.af.mil

ABSTRACT

Rolling element bearings are widely used in many mechanical systems and affect their safe operation and reliability. The use of an integral Oil Debris Monitoring (ODM) sensor in the lubrication system allows continuous monitoring of chips and particles originating from an evolving failure in the mechanical system oil wetted components.

This paper examines the use of the mass loss from an ODM sensor as a health indicator to assess damage severity and Remaining Useful life (RUL) of a rolling element bearing faulted in one of its raceways. A series of experiments were performed on a test rig using angular contact ball bearings subjected to high rotational speed and loads to study the propagation of a spall in the bearing raceway. A spall size estimation model that uses the mass loss from the ODM and known bearing characteristics was developed and showed good results. Based on tests results, a concept has been suggested to estimate bearing spall size and RUL to a critical spall size.

1. INTRODUCTION

Preventive Maintenance or Planned Maintenance (PM) are common maintenance policies where the machine is periodically inspected or replaced. The inspection or the replacement interval is predetermined by considering the reliability, maintainability, availability, and the machine safety.

Orel Portal et al. This is an open-access article distributed under the terms of the Creative Commons Attribution 3.0 United States License, which permits unrestricted use, distribution, and reproduction in any medium, provided the original author and source are credited.

The planned maintenance approach, relies on a routine time frame based upon many assumed factors such as reliable manufacturing process, inspection capabilities etc. Those assumptions lead to a compromise between availability and the machine safe operation. In the aviation industry the possibility for catastrophic event caused by mechanical system failure could lead to lack of availability and high financial costs and risk to the machine safety and perhaps human lives.

Condition Based Maintenance (CBM) is based on machine maintenance only when the need arises. This approach enables high system availability along with a reduction in maintenance costs. To enable the CBM approach, the capability to diagnose the machine health status is required. A damage severity and remaining useful life (RUL) assessment of all system components are required to determine maintenance scheduling.

One of the most common mechanical system components, are Rolling Element (RE) bearings, which carry load and allow relative motion between the bearing inner and outer rings. To reduce friction and wear on bearing components, most bearings are lubricated by oil or grease that also prolong the bearing fatigue life and prevent corrosion and contamination of the bearing. Many mechanical system manufacturers, integrate a closed loop lubrication system as part of their product. A well-known RE bearing damage is surface spalling, caused by rolling contact fatigue (Gazizulin, 2017).

Current bearing damage research is well established in the field of bearing damage diagnostics using vibration spectrum analysis and identification of bearing tones (Kass, Raad & Antoni, 2019). In the last years, some new studies on fault severity estimation of bearings were reported, but for our best

knowledge, studies on Remaining Useful Life (RUL) estimation were not published.

Examination of the machine lubrication oil to evaluate mechanical system health has been done for many decades (Joint Oil Analysis Program Manual Volume I, 2014). However, most methods require the use of off-line detection methodologies such as Oil Spectrometry inspections of Oil Filter, or Magnetic Chip Detector.

In recent years, ODM sensor-based machine health monitoring has become more common. The ODM sensor can detect particles in the machine oil lubrication system originating in oil wetted component such as gears and bearings by their size and type of material (Munir & Howe, 1996) by generating a magnetic field and measurement of the electromagnetic interference arising from particles passing through the oil system (Sun et al, 2021). Several papers have suggested the use of an ODM sensor to evaluate bearing damage severity (Forester, 2005). However, a validated ODM based model that enables bearing damage prognostics, prediction of damage severity throughout future use and RUL prediction has yet to be published.

This paper suggests the use of ODM sensor to predict bearing spall size as a health indicator for damage severity and a critical failure prognostics concept based on an ODM sensor. Chapter 2 contains a review on bearing spall propagation stages. In chapter 3, an ODM based model was suggested to estimate spall size. In chapter 4, endurance experiments used to investigate spall propagation behavior throughout the different propagation stages. Chapter 5 proposes a model that can be used for spall size prediction and chapter 6 summarizes this paper.

2. BACKGROUND

Spall growth in RE bearings can be divided into several stages. The first stage is the healthy bearing, where the spall has not been initiated yet. The initiation of a spall indicates the transition to stage two. The spall grows relatively slowly and locally, until it covers almost the entire width of the raceway (Bolander, 2009). Afterwards, the spall elongates across the race circumference. This initial elongation is characterized by a steady spall growth rate (Dempsey, Bolander et al, 2011). The final stage of the spall propagation is characterized by an increase in the rate of particle mass loss and particle count indicating a significant increase in the spall growth rate. Several articles suggested that this accelerated propagation stage starts when the spall length is equal roughly to the arc length between two adjacent rolling elements (Uluyol & Kim, 2010). The physical cause for the transition was recently explained by Madar et al. (2021). After the initiation, the spall geometry is generally amorphous and small relative to the raceway. In the later stages, the spall profile can be divided into an "entrance" region, a "bottom" region, and an "exit" region, where the width of the "bottom" region remains relatively constant

(Kass et al, 2019). Figure 1 shows the spall regions, and Figure 2 shows the typical propagation stages discussed.

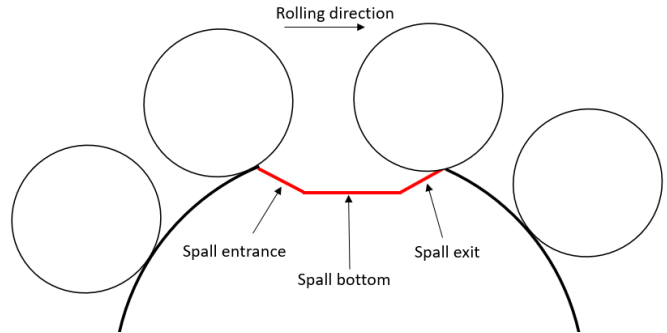


Figure 1. Inner raceway spall regions (spall not to scale) (Madar et al, 2021)

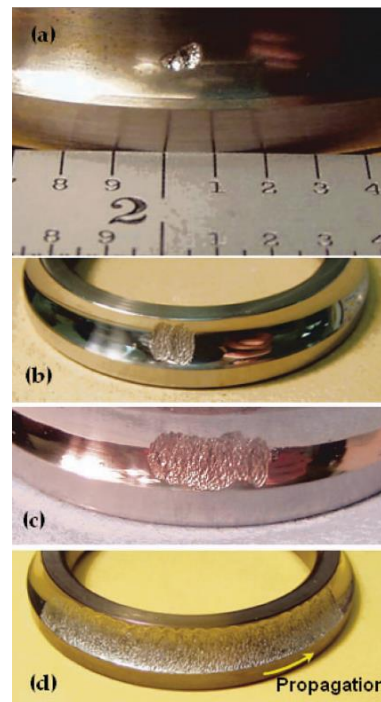


Figure 2. Typical spall propagation stage. (a) Initial spall. (b) Local spall widening. (c) Spall propagation. (d) accelerated spall propagation (Arakere et al, 2010)

3. DAMAGE SEVERITY MODEL BASED ON OIL DEBRIS

Previous research has suggested the length of the spall, or the spall angle, as a bearing damage indicator (Dupuis, 2010). When a spall is propagating on one of the bearing raceways, the spall length is related to the spall angle by the circumference. It is assumed that the spall geometry is mainly affected by the spall's "bottom" region and the spall width is roughly equivalent to the raceway width. By considering the contact area between the two elliptic bodies, as well as the geometry and the material properties, the maximum shear

stress depth can be calculated using Hertz contact theory. The total mass loss could be captured by an ODM sensor throughout the operation. The total mass loss is related to the raceway material density $\rho \left[\frac{mg}{mm^3} \right]$, a dimensionless calibration factor k and the spall volume $V[mm^3]$. For relatively large spalls, Madar et al. (2021) has shown that spall volume can be related to the spall length $L[mm]$ and a cross sectional area $A[mm^2]$. The cross-sectional area, A , can be expressed by the product of the spall depth $D[mm]$ and the spall width $W[mm]$. As previously mentioned, for relatively large spalls, the spall width is roughly the entire width of the raceway. Although the spall surface is not uniform, the average spall depth is found to be close to the maximum shear stress depth calculated by the Hertz contact theory. Thus, the spall depth is assumed to be the maximum Hertzian shear stress depth. These assumptions lead to the following relation between the spall length and the measured mass loss by the ODM sensor:

$$(1) \quad L[mm] = \frac{M[mg]}{k \cdot \rho \cdot D \cdot W}$$

Relatively large spall sizes, which are characterized by a spall whose width remain roughly constant and equal to the width of the raceway, could be estimated using this model. This estimation enables spall size assessment using only the known bearing geometry, material properties, and ODM sensor mass loss. However, for the early stages of spall propagation, a modification to the model is required to consider spall geometry that is smaller than the raceway width. A simple spall geometry model that could be suggested for this stage is a disk that grows in thickness until it covers the raceway width. The disk depth could be assumed to be the maximum shear stress depth by the Hertz contact theory. Once the spall disk covers roughly the entire raceway width, the addition to the spall length could be estimated using equation (1) as the spall grows only lengthwise along the raceway. A schematic concept for this early-stage ball geometry shown in Figure 3. The 1st stage represents a spall propagating as a disk until it covers the entire raceway. The 2nd stage represents a rectangular volume added onto the spall until the spall length is equal to arc length between two adjacent rolling elements.

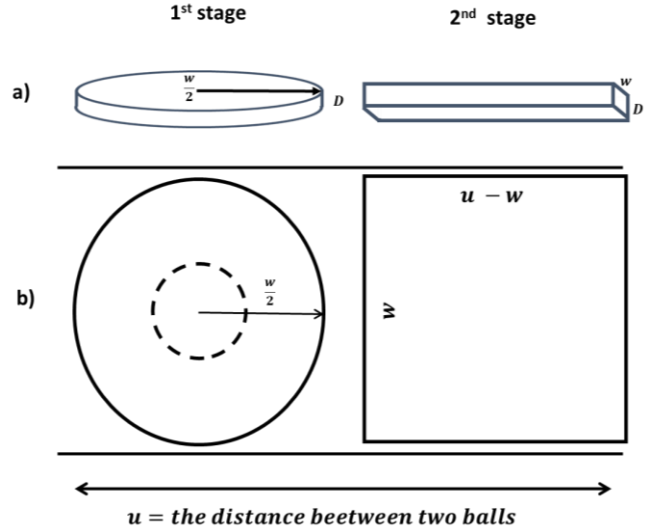


Figure 3. Concept schematic of early spall geometry a) 3D scheme across bearing raceway b) 2D scheme

4. RESULTS

Several controlled experiments were conducted in the United States Air Force Research Laboratories (AFRL) facility to explore spall propagation nature in angular contact AISI 52100 (AMS 6440) bearings with 13 AISI 2100 balls. The inner raceway was seeded with damage using hardness indentations to facilitate the initiation of an inner raceway spall. The bearing damage was monitored using an Oil Debris Monitoring (ODM) sensor. The experiment was conducted in two phases, spall initiation and spall propagation.

In the first phase of the experiment, each bearing was rotated at 10,000 RPM and subjected to 10kN of axial load until the test rig RMS vibration sensor crossed 2g threshold. This threshold is used by AFRL to ensure spall initiation is determined at similar sizes.

In the second phase, each bearing was rotated at the same rotating speed of 10,000 RPM, while the axial load was reduced to approximately 7.5kN to monitor damage propagation. This phase continued until the ODM sensor indicated a total mass loss of 1000mg. At the end of each phase, the bearing was disassembled from the test rig, all bearing components were weighed to evaluate the dimensionless calibration factor k mentioned in equation (1) and any observed damage was documented.

Eight bearings were tested. In the 1st experiment the mass loss indicated by the ODM sensor was extremely over-estimated relative to the actual mass loss. In the 4th test, the ODM sensor did not record the mass loss.

Figure 4 presents all the recorded cumulative mass loss from all the experiments except experiment 4 that was not recorded. In all the experiments, the transition between spall propagation stages could be noticed. After the initiation stage, spall growth occurs at a slow and relatively constant rate characterized by an approximately linear relationship between mass loss and time. Then an accelerated spall propagation growth occurs that is characterized by a rapid increase in the mass loss. In experiment 2, mass loss was rapidly accelerated relative to other experiments as two raceway spalls were found at the beginning of the slow propagation stage.

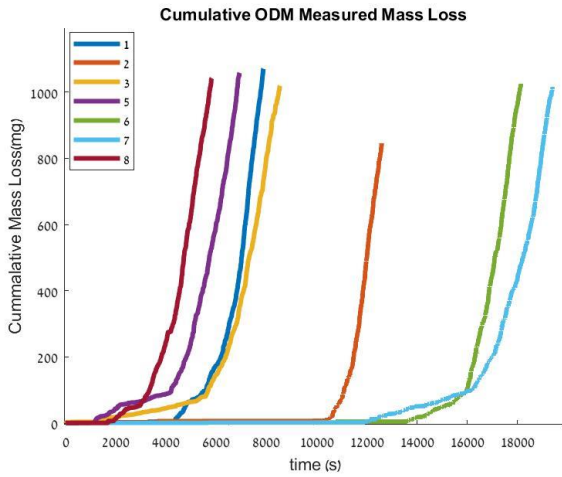


Figure 4. Estimated ODM mass loss versus time.

Figure 5 shows the relative particle size distribution every 10 mg of mass loss versus ODM mass loss. Figure 5a shows the distribution in experiment 3 and Figure 5b presents the distribution for the 6th experiment. Vertical lines mark the transition between the propagation stages, end of spall initiation stage at about 10 mg of mass loss and spall accelerated propagation stage at about 100 mg of mass loss. It could be noticed that particle size distribution is similar through damage propagation. Similar distributions were found in all experiments as the particle distribution is maximal for particles of 200 μm .

Previous research [9], estimated the spall angle at the end of each experiment using the geometry model based on equation (1) and has shown good results as the estimation spall angle was found within 13% of the measured spall angle at the end of each experiment. The assumptions made in this model are appropriate in the accelerated spall propagation stage. Where the spall covers roughly the entire width of the raceway and then propagates lengthwise.

To estimate smaller spalls, corresponding to the beginning of the spall propagation, the model should address spall volumes that are smaller than the width of the raceway. For example, a spall growing as a disk until it reaches the raceway width as suggested in chapter 4.

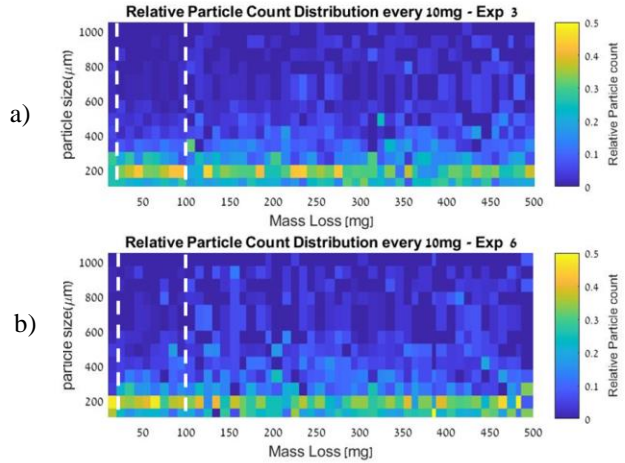


Figure 5: Relative particle size distributions every 10 mg of mass loss versus oil debris mass loss: a) Experiment 3, b) Experiment 6. Vertical lines represent the transition between spall propagation stages.

This model was used to estimate the spall size at the transition to the accelerated mass loss stage ("Knee Point") during the experiments. The error was calculated relative to the arc length between two adjacent balls which was calculated to be 12.2mm. The 1st stage disk depth was assumed to be the Hertzian maximum shear stress depth calculated to be 74 microns at initiation loads and 66.5 micron at propagation loads. The disk geometry grows until the spall covers the entire race width of 9.5mm. Afterwards, a box geometry was added with maximum shear stress depth dimension and race width dimension until the total geometries spall length was equal to the arc length between two adjacent balls. The ODM sensor calibration factor was found to be relatively similar for all the experiments with a value of 1.6 and the bearing inner race 52100 (AMS 6440) material density is $7.8 \frac{mg}{mm}$. The average spall size estimation error was found was about 5% as shown in Table 1. Estimation of the 4th experiment is missing due to ODM sensor not recording.

# Experiment	Estimated Spall Length [mm]	Error [%]
1	11.81	3.18
2	11.74	3.77
3	11.76	3.58
5	11.21	8.15
6	11.57	5.17
7	13.05	7.00
8	11.97	1.88
Average	11.16	4.67

Table 4. Estimated spall size at the "Knee Point."

5. PROGNOSTICS BASED ON OIL DEBRIS

Incorporating an ODM sensor into a machine, allows monitoring oil system debris originating from all oil wetted components. The mass loss is directly related to the spall volume which under certain spall geometry assumptions is related to the spall size and severity. Therefore, cumulative mass loss could act as a good health indicator to damage propagating in a bearing due to its monotonic behavior and the physical relation between the mass loss and the size of the bearing spall.

An ODM sensor alone cannot diagnose which machine component is faulted, as debris caught by the ODM sensor could originate from different components in the machine. In rotating machinery, identification of the faulty component can be achieved by vibration analysis. However, once the faulty bearing has been identified, ODM sensors allow bearing damage severity estimation and damage prognostics.

Total cumulative mass loss along with the known bearing geometry and material properties, allow estimation of the spall size even in the early stages of the spall propagation. Assuming the critical spall size is smaller than the arc length between two adjacent balls and occurs prior to the transition from the constant propagation to the accelerated spall propagation phases, prognostics could be made to estimate the bearing Remaining Useful Life (RUL).

Figure 6 shows the 3rd experiment cumulative mass loss versus operation time starting from spall initiation up to the accelerated spall propagation stage. It can be observed that there is a linear behavior of the mass loss through time.

Using the spall geometry model that assumes an initial spall disk until the spall covers the raceway width, and then add a box volume for additional spall length, the cumulative mass loss and spall geometry can be used to estimate the spall size. Assuming constant rotating speed and load, a constant mass loss rate is expected during early spall propagation stages before the “Knee Point”. This allows Remaining Useful Life (RUL) assessment up to a critical spall size below the arc length between two adjacent rolling elements.

There are several factors contributing to uncertainty of the ODM measurements, such as delay in detection of particles, inaccurate estimation of each particle mass and quantization of particles dimensions. In addition, the bearing in a real machine is not operated under constant conditions that could change considerably. The assumed geometry model is simplified and introduce uncertainty in the estimation of the spall size. Quantitative uncertainty evaluation is the subject of future study that will require experiments providing correlation between spall size, vibrations and ODM.

ODM based RUL estimation will assume a linear propagation of the spall size that should be applied after identification of the bearing fault initiation based on vibration analysis and will be continuously updated to improve the RUL accuracy and to fit changing operating conditions.

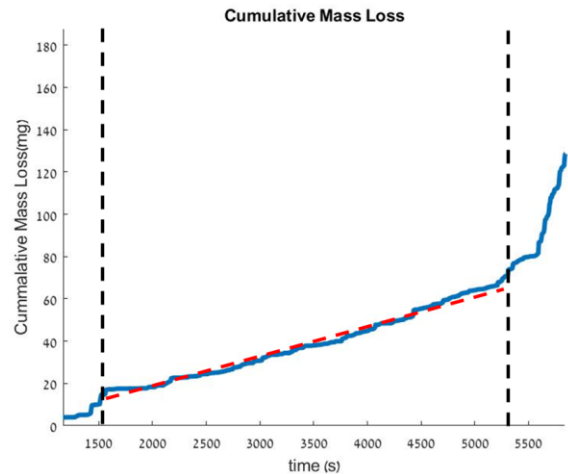


Figure 6: Experiment 3 mass loss versus time. Black vertical lines represent the transition between spall propagation stages. Red dotted line represents early propagation at constant mass loss behavior before transition to accelerated propagation stage.

6. SUMMARY AND CONCLUSIONS

Assessment of spall severity on one of the bearing raceways based on the mass loss collected by an oil debris sensor and a spall geometry changing with the failure progression has been suggested. Several endurance experiments were performed with angular contact AISI 52100 bearings to examine mass loss debris and particle size distribution throughout the fault growth. The particle size distribution was found to be constant throughout the fault progression. A linear relation has been found between the mass loss and operation time at early spall propagation stages, prior to the accelerated propagation stage. A spall geometry model has been developed to estimate bearing spall size and has shown good results of about 5% average error relative to the analytical value. A concept has been suggested to estimate the Remaining Useful Life (RUL) for critical spalls that cover an angle smaller than the angle between two adjacent balls. This concept requires an indication on the presence of the fault in a specific location or bearing and therefore depends on other health monitoring techniques such as vibration analysis to identify the fault location. Moreover, more research is needed to develop and validate robust diagnostics and prognostics based on a combination of ODM data and vibrations, as well as uncertainty management.

References

- Gazizulin D, Klein R, Bortman J. (2017). Towards efficient spall generation simulation in rolling element bearing. *Fatigue Fract Eng Mater Struct* 40 :1389–405. <https://doi.org/10.1111/ffe.12580>.
- Kass, S., A. Raad, and J. Antoni. (2019). “Self-Running Fault Diagnosis Method for Rolling Element Bearing.” *Mechanisms and Machine Science* 58(March):127–40.
doi: 10.1007/978-3-319-89911-4_10
- Joint Oil Analysis Program Manual (2014) Volume I, US AIR FORCE T.O 33-1-37-1, 15-Sep-2014
- Bolander N, Qiu H, Eklund N, Hindle E, Rosenfeld T. (2009) Physics-based remaining useful life prediction for aircraft engine bearing prognosis. *Annual Conference of Health Management Society* vol. 1. 2009.
- Dempsey PJ, Bolander N, Haynes C, Toms AM. (2011) Investigation of Bearing Fatigue Damage Life Prediction Using Oil Debris Monitoring. *Nasa Tm-2011-217117* :18.
- Uluyol O, Kim K, Hickenbottom C. (2010) A systematic approach to bearing health monitoring. *Annu Forum Proc - AHS Int* ;3:2464–76.
- Cassidy K. MetalSCAN - Qualification of an On-Line Bearing and Gear Health Monitoring Technique for In-Service Monitoring of Aircraft Engines and Helicopter Transmissions n.d.
- Madar, E., Galiki, O., Klein, R., Bortman, J., Nickell, J., & Kirsch, M. (2021). A New Model for Bearing Spall Size Estimation Based on Oil Debris. *Engineering Failure Analysis*, 106011.
- Arakere NK, Branch N, Levesque G, Svendsen V, Forster NH. (2010). Rolling contact fatigue life and spall propagation of AISI M50, M50NiL, and AISI 52100, part II: Stress modeling. *Tribol Trans* ;53:42–51. <https://doi.org/10.1080/10402000903226325>.
- Dupuis R. (2010) Application of Oil Debris Monitoring For Wind Turbine Gearbox Prognostics and Health Management.
- Muir D. Howe B. (1996) In-Line Oil Debris Monitor (ODM) For The Advanced Tactical Fighter Engine.
- Sun J, Wang L, Li J, Li F, Li J, Lu H. (2021) Online oil debris monitoring of rotating machinery: A detailed review of more than three decades. *Mech Syst Signal Process* 2021;149:107341. <https://doi.org/10.1016/j.ymsp.2020.107341>.
- Forster et al. (2005). “Assessing the Potential of a Commercial Oil Debris Sensor as a Prognostic Device for Gas Turbine Engine Bearings” Forster N.H., Thompson K., Toms A.M., Horning S. *AFRL presentation at ISHM conference, August 2005, Cincinnati, OH*
- Hong W. et al. (2009) A Novel Indicator for Mechanical Failure and Life Prediction Based on Debris Monitoring. *IEEE Transactions on Reliability* 99: 1-9.